J Am Soc Nephrol 13: 875–886, 2002

Differential Expression Patterns of Claudins, Tight Junction Membrane Proteins, in Mouse Nephron Segments

YUMIKO KIUCHI-SAISHIN,*† SHIMPEI GOTOH,* MIKIO FURUSE,* AKIKO TAKASUGA,‡ YASUO TANO,† and SHOICHIRO TSUKITA*

**Department of Cell Biology, Kyoto University Faculty of Medicine, Kyoto, Japan; †Department of Ophthalmology, Osaka University Medical School, Osaka, Japan; and ‡Shirakawa Institute of Animal Genetics, Fukushima, Japan.*

Abstract. As the first step in understanding the physiologic functions of claudins (tight junction integral membrane proteins) in nephrons, the expression of claudin-1 to -16 in mouse kidneys was examined by Northern blotting. Among these claudins, only claudin-6, -9, -13, and -14 were not detectable. Claudin-5 and -15 were detected only in endothelial cells. Polyclonal antibodies specific for claudin-7 and -12 were not available. Therefore, the distributions of claudin-1, -2, -3, -4, -8, -10, -11, and -16 in nephron segments were examined with immunofluorescence microscopy. For identification of individual segments, antibodies specific for segment markers were used. Immunofluorescence microscopic analyses of serial frozen sections of mouse kidneys with polyclonal antibodies for claudins and segment markers revealed that claudins demonstrated very complicated, segment-specific, expression patterns in nephrons, *i.e.*, claudin-1 and -2 in Bowman's capsule, claudin-2, -10, and -11 in the proximal tubule, claudin-2 in the thin descending limb of Henle, claudin-3, -4, and -8 in the thin ascending limb of Henle, claudin-3, -10, -11, and -16 in the thick ascending limb of Henle, claudin-3 and -8 in the distal tubule, and claudin-3, -4, and -8 in the collecting duct. These segment-specific expression patterns of claudins are discussed, with special reference to the physiologic functions of tight junctions in nephrons.

In multicellular organisms, epithelial cellular sheets not only function as diffusion barriers, to establish compositionally distinct fluid compartments, but also are involved in active transport of materials across the barrier, to dynamically maintain the internal environment of each compartment. For cellular sheets to exert these physiologic functions, there must be some seal to the diffusion of solutes through the paracellular pathway. Tight junctions (TJ) have been demonstrated to be responsible for this intercellular sealing (1–3). Morphologic and physiologic studies, however, have revealed that TJ are not simple barriers; they demonstrate ion and size selectivity, and their barrier function varies significantly in tightness, depending on the cell type and physiologic requirements (4,5). Such regulated diversified permeability of TJ is thought to be required for dynamic maintenance of the interior environment of each compartment.

With ultrathin-section electron microscopy, TJ appear as a series of discrete sites of apparent fusion, involving the outer leaflet of the plasma membranes of adjacent cells (6). With freeze-fracture electron microscopy, TJ appear as a set of continuous, anastomosing, intramembranous particle strands (TJ strands) (7,8). These morphologic findings led to the following structural model for TJ: within the lipid bilayer of each membrane, the TJ strands, which are probably composed of linearly aggregated integral membrane proteins, form networks through their ramifications (3). TJ strands laterally and tightly associate with strands in the apposing membranes of adjacent cells to form paired strands, where the intercellular distance becomes almost zero.

Two distinct types of integral membrane proteins have been identified as components of TJ strands, namely occludin and claudins (9,10). Both occludin and claudins have four transmembrane domains, but they demonstrate no sequence similarity with each other. Claudins, with molecular masses of approximately 23 kD, comprise a multigene family consisting of >20 members (3,10–12). When each claudin species or occludin was overexpressed in mouse L fibroblasts, claudin molecules, but not occludin, were polymerized within the plasma membranes to reconstitute paired TJ strands, indicating that claudins are major structural components of TJ strands (13). It was recently demonstrated that heterogeneous claudin species are copolymerized to form individual TJ strands as heteropolymers and that, between adjacent TJ strands, claudin molecules adhere to each other in both homotypic and heterotypic manners, except in some combinations (14). Importantly, detailed analyses suggested that variations in the tightness of individual paired TJ strands are determined by the combinations and mixing ratios of claudin species (3,15–17).

The kidney is composed of numerous nephrons, which are delineated by epithelial cellular sheets. Each nephron has several segments, which differ in histologic structure and function. Nephrons are directly involved in the production of urine via

Received August 7, 2001. Accepted November 22, 2001.
Correspondence to Dr. Shoichiro Tsukita, Department of Cell Biology, Kyoto University Faculty of Medicine, Konoe-Yoshida, Sakyo-ku, Kyoto 606, Japan. Phone: 81-75-753-4372; Fax: 81-75-753-4660; E-mail: htsukita@mfour.med.kyoto-u.ac.jp

1046-6673/1304-0875
Journal of the American Society of Nephrology

collection of the blood filtrate, addition of metabolic waste, and reabsorption of components that need to be conserved. Therefore, these compartments (*i.e.*, nephrons) are essential for the physiologic functions of the kidney. TJ play a central role in this compartmentalization, and the tightness of TJ varies significantly, depending on the nephron segment. As mentioned above, claudins have been identified as structural as well as functional components of TJ strands. Therefore, as the first step in understanding the functions of TJ in individual nephron segments in molecular terms, it is necessary to determine which types of claudins are expressed in each segment. Interestingly, mutations in the gene encoding claudin-16/paracellin-1, which is expressed in the thick ascending limb of Henle, were reported to affect the resorption of magnesium ions from the urine, resulting in human hereditary hypomagnesemia (16).

In this study, we systematically examined the expression patterns of claudins (claudin-1 to -16) in each mouse nephron segment. Although the expression and distribution of several claudin species remain undetermined because of the lack of available antibodies, this study demonstrated the complicated patterns of segment-specific expression of claudin species in nephrons. The results presented here are important for future physiologic studies of nephron functions.

Materials and Methods

Antibodies

Rabbit anti-mouse polyclonal antibodies (pAb) to claudin-2, -3, -4, -5, -8, and -11 and rat anti-mouse occludin monoclonal antibody (mAb) were raised and characterized as described previously (11,14,18–20). Rabbit anti-rat aquaporin-2 (AQP2) pAb was kindly provided by Dr. Sei Sasaki (Tokyo Medical and Dental University, Tokyo, Japan). Rabbit anti-claudin-1 pAb, rabbit anti-Tamm-Horsfall glycoprotein (THP) pAb, and rabbit anti-chloride channel-K (ClC-K) pAb were purchased from Zymed Laboratories (South San Francisco, CA), Biomedical Technologies (Stoughton, MA), and Alomone Laboratories (Jerusalem, Israel), respectively. Rabbit anti-AQP1 pAb was purchased from Chemicon International (Temecula, CA).

For generation of anti-claudin-10 pAb in rabbits, a glutathione *S*-transferase (GST) fusion protein with the carboxy-terminal cytoplasmic domain of mouse claudin-10, which was produced in *Escherichia coli* (strain DH5a) and purified with glutathione-Sepharose 4B beads (Amersham-Pharmacia Biotech., Bucks, UK), was used as an antigen. For generation of anti-claudin-7, -12, -15, and -16 pAb, polypeptides corresponding to the respective carboxy-terminal cytoplasmic domains of mouse claudin-7, -12, and -15 and bovine claudin-16 (21) were synthesized and coupled, via cysteine, to keyhole limpet hemocyanin. These conjugated peptides were used as antigens in rabbits. The pAb were affinity-purified on nitrocellulose membranes with the corresponding GST fusion proteins. During the generation of pAb, animal experiments were conducted in accordance with the National Institutes of Health *Guide for the Care and Use of Laboratory Animals*.

Northern Blotting

Total RNA from mouse kidneys was isolated according to the method described by Chomczynski and Sacchi (22). Poly(A)$^+$ RNA was obtained from total RNA by using oligo(dT)-cellulose beads (New England BioLabs, Beverly, MA). Aliquots of approximately 10 μg of poly(A)$^+$ RNA were separated on 1% formaldehyde/agarose gels, transferred to positively charged nylon membranes, and crosslinked with ultraviolet light. Hybridization with digoxigenin (DIG)-labeled RNA probes was performed according to the protocol described by the manufacturer (Roche, Mannheim, Germany). RNA probes were DIG-labeled using a DIG RNA labeling kit (Roche).

Sodium Dodecyl Sulfate-Polyacrylamide Gel Electrophoresis and Immunoblotting

Lysates of *E. coli* expressing a maltose-binding protein fusion protein with the cytoplasmic portion of mouse claudin-10 or GST fusion proteins with the cytoplasmic portions of the other mouse claudin species were subjected to one-dimensional sodium dodecyl sulfate-polyacrylamide gel electrophoresis (12.5%), according to the method described by Laemmli (23), and gels were stained with Coomassie Brilliant Blue R-250. For immunoblotting, proteins were electrophoretically transferred from gels to nitrocellulose membranes, which were then incubated with the first antibody. Bound antibodies were detected with biotinylated second antibodies and streptavidin-conjugated alkaline phosphatase (Amersham Corp., Arlington Heights, IL). Nitroblue tetrazolium and bromochloroindolyl phosphate were used as substrates for detection of alkaline phosphatase activity.

Immunofluorescence Microscopy

Kidneys were removed from mice and frozen with liquid nitrogen. For staining with anti-claudin-1 pAb, kidneys were fixed for at least 2 h with 4% paraformaldehyde in phosphate-buffered saline (PBS) (pH 7.2), immersed for 48 h in PBS containing 15% sucrose, and then frozen with liquid nitrogen. For TCA fixation (24), small pieces of kidney were soaked in ice-cold 10% TCA for 1 h, washed three times with PBS, and then frozen with liquid nitrogen. Pairs of serial frozen sections (approximately 10 μm thick) were cut with a cryostat, mounted on single glass slides, and air-dried. Sections were then fixed with 95% ethanol at 4°C for 30 min, followed by 100% acetone at room temperature for 1 min. After soaking in PBS containing 1% bovine serum albumin (and 0.2% Triton X-100 for claudin-1 staining only), one of the sections was incubated with one of the anti-claudin pAb (or preimmune serum) and the other was treated with one of the segment marker-specific pAb, in a moist chamber, for 30 min. For control experiments, anti-claudin pAb were preincubated with excess amounts of GST fusion proteins with the cytoplasmic domains of the respective claudins. Sections were then washed three times with PBS, followed by a 30-min incubation with secondary antibodies. Cy3-conjugated and FITC-conjugated secondary antibodies were used for the anti-claudin pAb-treated and anti-segment marker pAb-treated sections, respectively. After being washed with PBS, sections were embedded in 95% glycerol/PBS containing 0.1% *p*-phenylendiamine and 1% *n*-propyl gallate and were observed with a fluorescence microscope (Axiophot photomicroscope; Carl Zeis, Inc., Thornwood, NY) equipped with a cooled, charge-coupled device camera system.

Results

Expression of Claudin Isotypes in the Kidney

We first examined the expression of claudin-1 to -16 in mouse kidneys by Northern blotting. When the poly(A)$^+$ RNA isolated from the kidneys was probed with DIG-labeled mouse claudin-1 to -16 RNA, the expression of most claudin species was clearly detected, whereas claudin-6, -9, -13, and -14 were not detected (Figure 1A). Because claudin-6, -9, -13, and -14 mRNA were clearly detected with the same probes in other

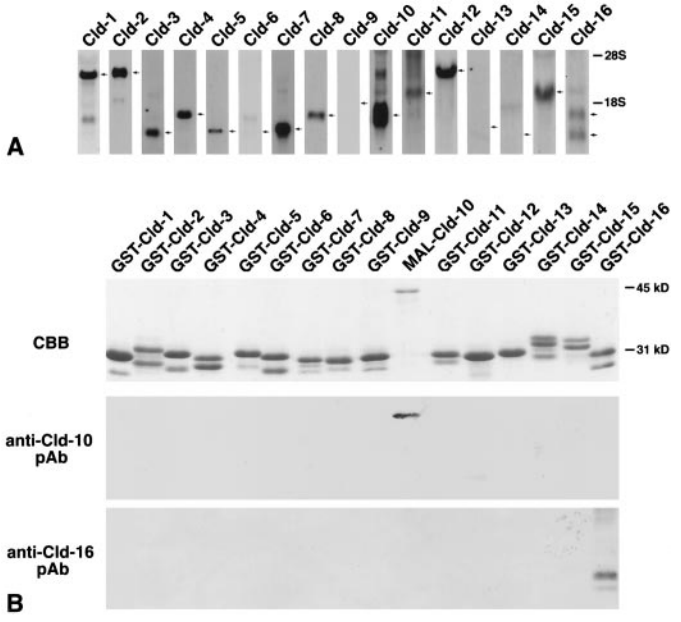

Figure 1. (A) Northern blots of mouse claudin-1 to -16 (Cld-1 to -16) expression in the kidney. Claudin-6, -9, -13, and -14 were undetectable. Arrows, positions of individual claudin mRNA expected from Northern blotting analyses of other tissues, such as the liver. (B) Specificity of newly generated anti-claudin-10 and -16 polyclonal antibodies (pAb). Immunoblotting of total lysates of *Escherichia coli* expressing glutathione *S*-transferase (GST) (or maltose-binding protein [MAL]) fusion proteins with cytoplasmic domains of claudin-1 to -16 confirmed the specificities. CBB, Coomassie Brilliant Blue staining; anti-Cld-10 pAb, immunoblotting with anti-claudin-10 pAb; anti-Cld-16 pAb, immunoblotting with anti-claudin-16 pAb.

tissues, we concluded that the expression levels of claudin-6, -9, -13, and -14 were fairly low in mouse kidneys.

Next, to examine the distributions of individual claudins expressed in the kidney, we prepared antibodies specific for all of these claudins. Anti-claudin-1 pAb was purchased from Zymed Laboratories. pAb to claudin-2, -3, -4, -5, -8, and -11 were raised and characterized previously (11,14,18,19). We then produced GST fusion proteins or synthesized polypeptides from the cytoplasmic tails of the other claudins (claudin-7, -10, -12, -15, and -16) and raised pAb using those proteins or polypeptides as antigens. The pAb for claudin-10, -15, and -16 worked well for both immunoblotting and immunofluorescence microscopic analyses but, despite intensive efforts, we failed to obtain pAb for claudin-7 or -12 that could be used for immunofluorescence microscopy. Therefore, we have no information regarding the distributions of claudin-7 and -12 in nephrons. Furthermore, because claudin-5 and -15 were expressed specifically in endothelial cells of blood vessels, we do not discuss the expression or distribution of these claudins in the kidney in detail in this report. The specificities of newly generated anti-claudin-10 and -16 pAb were demonstrated by Western blotting analyses of total lysates of *E. coli* expressing GST fusion proteins with the cytoplasmic domains of claudin-1 to -16 (Figure 1B). As previously demonstrated (11,25), it was technically difficult to evaluate the specificities of anti-claudin pAb in Western blotting analyses of total lysates of whole organs, mainly because the levels of expressed claudins were fairly low.

Segment-Specific Expression of Claudin-8 in Nephrons

To identify individual nephron segments with immunofluorescence microscopy, we used antibodies to several segment markers (Figure 2). The proximal tubules and the thin descending limb of Henle were identified as AQP1-positive tubules in the cortex and the medulla, respectively (26). The thin and thick ascending limbs of Henle in the medulla were distinguished by the expression of ClC-K (27,28) and THP, respectively (29). The anti-ClC-K pAb used in this study recognized both ClC-K1 and ClC-K2, but in the medulla only the thin ascending limb of Henle was reported to express ClC-K1 (not ClC-K2) (27,28). Because the collecting tubules were reported to be positive for AQP2 (30), the distal tubules were identified as AQP1/2-double-negative tubules located around glomeruli.

We then immunofluorescently stained serial frozen sections from the mouse kidneys with pAb for each claudin species or with pAb for the segment markers. This method indicated that individual claudin species exhibit specific patterns of expression in nephron segments. The segment-specific expression of claudin-8 is demonstrated in Figure 3, as an example. In the cortex, claudin-8 was expressed and concentrated at junctional regions (probably TJ) in some but not all tubules. The AQP1-positive tubules lacked claudin-8 expression, whereas all of the AQP2-positive tubules expressed claudin-8, indicating that claudin-8 is expressed in collecting ducts but not in proximal tubules. The TJ-specific concentration of claudin-8 was also detected in the AQP1/2-double-negative tubules located around glomeruli, indicating the expression of claudin-8 in distal tubules. In the medulla, some tubules exhibited a concentration of claudin-8 at TJ. These tubules were ClC-K-positive but AQP1/THP-negative, leading to the conclusion that claudin-8 was expressed exclusively in the thin ascending limb of Henle in the medulla.

To evaluate these segment-specific staining patterns, we performed the following control staining experiments (Figure 4). First, frozen sections were double-stained with anti-occludin mAb and anti-claudin-8 pAb, to confirm that claudin-8 signals were derived from TJ. Second, sections were stained with preimmune serum. Third, sections were stained with anti-claudin-8 pAb in the presence of GST-claudin-8 or GST-claudin-5, to evaluate the specificity of the staining with anti-claudin-8 pAb. Using this type of analysis, with similar control staining experiments, we examined in detail the segment-specific expression of other claudin species in nephrons, as described below.

Distinct Patterns of Expression of Claudins in Nephron Segments

Bowman's Capsule. To examine whether certain claudin species are expressed in Bowman's capsule, we compared phase-contrast images of frozen sections with the corresponding immunofluorescence microscopic images obtained by using specific pAb. As demonstrated in Figure 5A, claudin-1 and

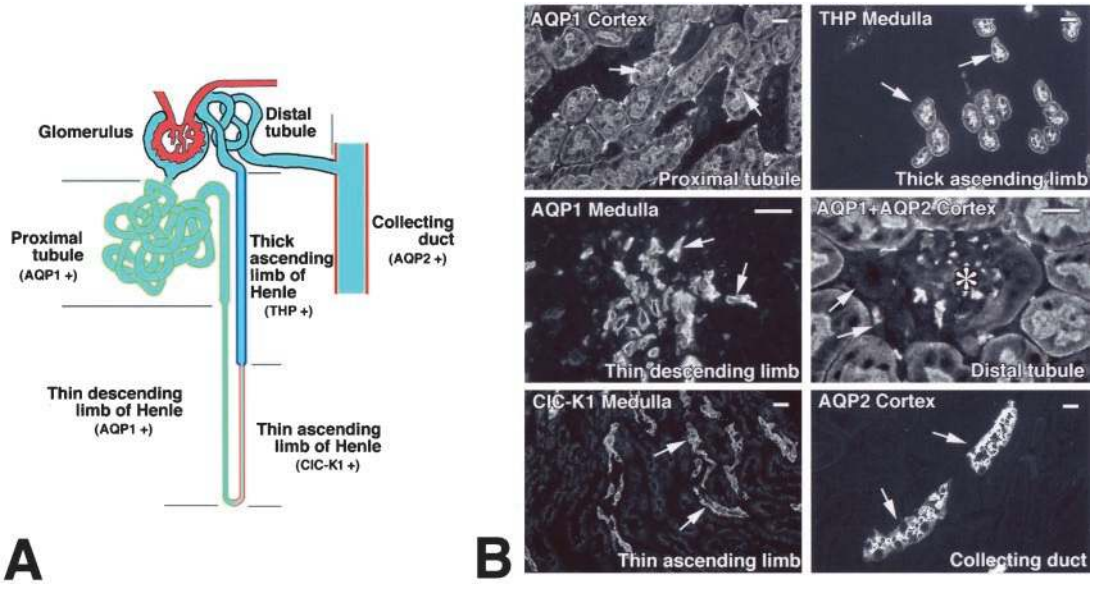

Figure 2. Identification of nephron segments with fluorescence microscopy. (A) Nomenclature for nephron segments used in this study. (B) Segment markers. Frozen sections of mouse kidneys were immunofluorescently stained with pAb for each segment marker. The proximal tubules and the thin descending limbs of Henle were identified as aquaporin-1 (AQP1)-positive tubules in the cortex and medulla, respectively. The thin and thick ascending limbs of Henle in the medulla were distinguished by the expression of chloride channel-K1 (ClC-K1) and Tamm-Horsfall glycoprotein (THP), respectively. The distal tubules were identified as AQP1/2-double-negative tubules located around glomeruli (asterisk), and the collecting tubules were identified as AQP2-positive tubules. Arrows, tubules identified by segment markers. Bars, 20 μm.

-2 were concentrated at the borders of epithelial cells of Bowman's capsule. We noted that the claudin-1 pAb (Zymed Laboratories) recognized not only claudin-1 but also claudin-3. To evaluate the staining of Bowman's capsule with anti-claudin-1 pAb, we stained the kidneys of claudin-1-deficient mice (Furuse M, Hata M, Tsukita SH; unpublished data) with this antibody. In those mice, no signal was detected for Bowman's capsule, indicating that claudin-1 is specifically expressed, together with claudin-2, in the capsule.

Proximal Tubule. Claudin-2, -10, and -11 were clearly concentrated at TJ of epithelial cells of AQP1-positive tubules in the cortex, *i.e.*, the proximal tubules (Figure 5B). Among these, only claudin-2 seemed to be distributed along basal plasma membranes in addition to TJ. This staining was specific for claudin-2, because the kidneys of claudin-2-deficient mice demonstrated no such staining (Furuse M, Hata M, Tsukita SH; unpublished data).

Thin Descending Limb of Henle. Only claudin-2 was detected in most of the AQP-1-positive tubules in the medulla, *i.e.*, the thin descending limb of Henle (Figure 6). Under the fixation conditions used in this study, claudin-2 did not seem to be concentrated in TJ-like thin lines but was diffusely distributed in broad bands. This characteristic staining was absent with preimmune serum; very strangely, when sections were doubly stained with anti-occludin mAb and anti-claudin-2 pAb, not only claudin-2 but also occludin seemed to be diffusely distributed in broad bands. This staining became undetectable when anti-claudin-2 pAb was pretreated with GST-claudin-2, and staining was not observed in claudin-2-deficient mouse kidneys (data not shown). These findings suggested that the diffuse distribution of claudin-2 in the thin descending limb of Henle was specific.

Then, to improve the preservation of fixed tubules, we applied the newly developed TCA fixation method (24) (Figure 6). Similar diffuse claudin-2 staining was detected at low magnification, but close inspection revealed that individual sharp lines were intermingled within the claudin-2-positive bands. These lines were also Zomula Occludens-1-positive (occludin-positive). Because the constituent cells in the thin descending limb of Henle are very flat and are interdigitated in a very complex manner (31), it is safe to conclude that claudin-2 was concentrated specifically at TJ in this segment.

Thin Ascending Limb of Henle. In addition to claudin-8 (Figure 3), claudin-3 and -4 were concentrated at TJ of epithelial cells of ClC-K-positive tubules in the medulla, *i.e.*, the thin ascending limb of Henle (Figure 7).

Thick Ascending Limb of Henle. Four distinct species of claudins, namely claudin-3, -10, -11, and -16, were detected at TJ of epithelial cells of THP-positive tubules in the medulla, *i.e.*, the thick ascending limb of Henle (Figure 8). In the cortex of some species, including mice, THP has been reported to be expressed also in the distal tubules (32); however, among claudin-3, -10, -11, and -16, only claudin-3 staining was positive in the distal tubules, as demonstrated below. Because the frozen sections were not very thin, these claudin-positive lines frequently seemed to correspond to apical surfaces, but detailed double staining of transversely sectioned tubules with

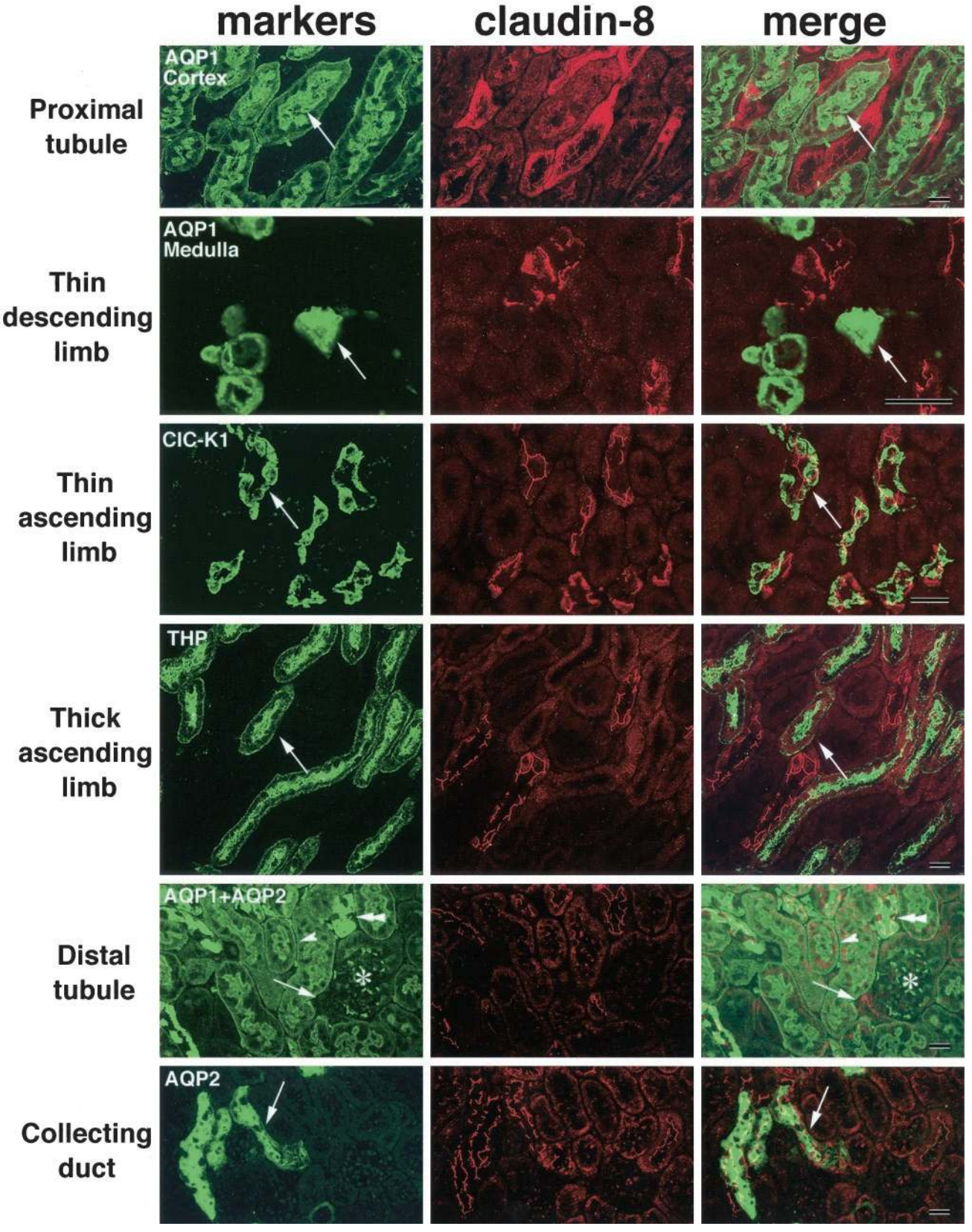

Figure 3. Segment-specific expression pattern of claudin-8 in nephrons. One of each pair of serial frozen sections was stained with pAb for segment markers in green (markers), and the other was stained with anti-claudin-8 pAb in red (claudin-8). These two images were then merged (merge). This analysis revealed that claudin-8 was concentrated at tight junctions (TJ) in epithelial cells of the thin ascending limb of Henle, the distal tubule, and the collecting duct. Arrows, tubules identified with segment markers; arrowhead, proximal tubule; double arrowhead, collecting duct; asterisks, glomeruli. Bars, 20 μm.

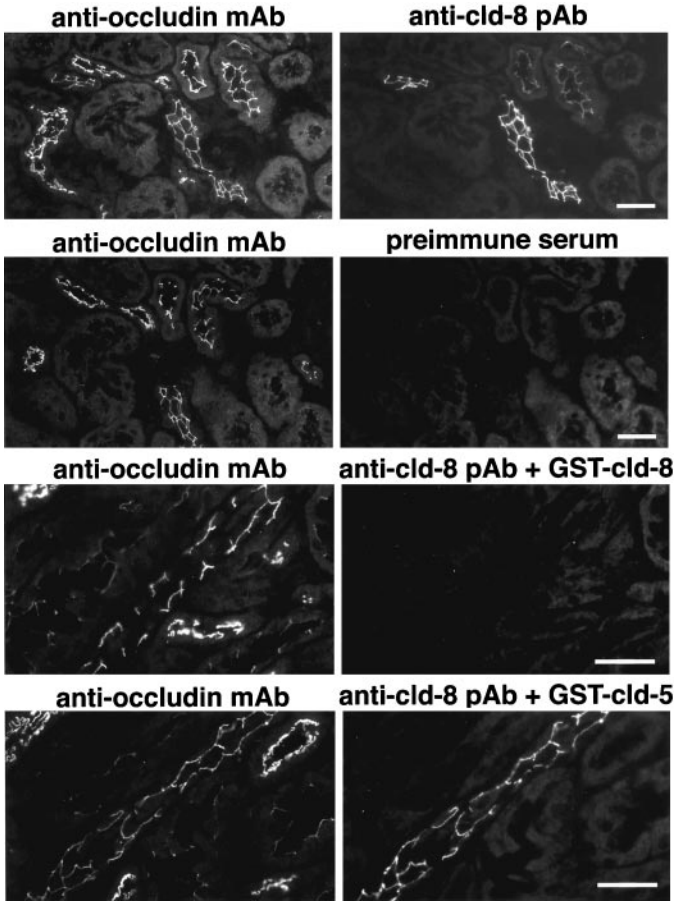

Figure 4. Specificities of anti-claudin-8 (anti-cld-8) pAb in immunofluorescence microscopic analyses. When the frozen sections were double-stained with anti-occludin monoclonal antibody (mAb) and anti-claudin-8 pAb, in some types of tubules (Figure 3) claudin-8 appeared to be concentrated in lines, which precisely coincided with the occludin-positive TJ. These claudin-8-positive lines were undetectable with preimmune serum or with anti-claudin-8 pAb pretreated with GST-claudin-8. Pretreatment with GST-claudin-5 did not affect the staining ability of anti-claudin-8 pAb. Bars, 20 μm.

anti-occludin mAb clearly revealed that these lines corresponded to TJ, not to apical surfaces (Figure 8, insets).

Distal Tubule. As demonstrated above, the distal tubules were identified as AQP1/2-double-negative tubules around glomeruli. In this type of tubule, claudin-3 (Figure 9A) and -8 (Figure 3) were expressed and localized at TJ.

Collecting Duct. In addition to claudin-8 (Figure 3), claudin-3 and -4 were clearly detected at TJ of epithelial cells of AQP2-positive tubules, *i.e.*, collecting tubules (Figure 9B). These segment-specific expression patterns of claudins in nephrons are summarized in Figure 10.

Discussion

To date, >20 members of the claudin family have been identified, but our knowledge regarding the expression patterns of these claudin species in individual organs is still fragmentary. Because the kidney has a complicated epithelial cell architecture, we expected to observe the coexpression of several claudin species in this organ. Surprisingly, Northern blotting revealed that, of the 16 species of claudins investigated (claudin-1 to -16), 12 distinct species were expressed in the kidney. More importantly, immunofluorescence microscopy revealed that these claudins demonstrated segment-specific expression patterns in nephrons, except for claudin-5 and -15, which were expressed in endothelial cells; antibodies specific for claudin-7 and -12 were not available. Therefore, questions have naturally arisen regarding the physiologic relevance of such complicated patterns of segment-specific expression of various claudin species in nephrons.

Several distinct types of claudins have been reported to be coexpressed in other types of cells, such as hepatocytes (14) and intestinal epithelial cells (33). In those cells, heterogeneous claudin species are thought to be copolymerized into individual TJ strands; within paired strands, claudins adhere to each other in homotypic as well as heterotypic manners (14). Several lines of evidence recently suggested that the combinations and mixing ratios of claudins within individual paired strands determine their tightness (3,17). Therefore, the distinct patterns of expression of claudins in nephron segments may be involved in the diversity of the paracellular flux in various segments. The following two recent observations seem to favor this suggestion.

There are two strains of the cultured epithelial cell line established from dog kidneys, *i.e.*, MDCK I and II cells. MDCK I cells demonstrate much higher transepithelial electric resistance than do MDCK II cells, although the strains bear similar numbers of TJ strands (34). The expression patterns of claudins in these cells were recently reported (15). Claudin-1 and -4 were expressed in both MDCK I and II cells, whereas the expression of claudin-2 was restricted to MDCK II cells. Dog claudin-2 cDNA was then introduced into MDCK I cells, to mimic the claudin expression pattern of MDCK II cells. Interestingly, the transepithelial electric resistance values of MDCK I clones stably expressing claudin-2 decreased to the levels of MDCK II cells (>20-fold decrease). These findings indicated that the addition of claudin-2 markedly decreased the tightness of individual TJ strands. As summarized in Figure 10, claudin-2 was specifically concentrated in TJ of the proximal tubules and Bowman's capsule in the kidney, and it is well known that TJ in proximal tubules are fairly leaky (35,36). Therefore, it is tempting to speculate that claudin-2 plays an important role in keeping TJ of proximal tubules leaky, although it is also known that the number of TJ strands in proximal tubules is less than that in distal tubules (37).

The second observation was made among patients with hereditary hypomagnesemia (16). The renal resorption of Mg^{2+} occurs predominantly via the paracellular pathway in the thick ascending limb of Henle, but in these patients this paracellular flux is blocked, resulting in severe hypomagnesemia. Positional cloning identified claudin-16/paracellin-1 as the gene responsible for this disease. Interestingly, claudin-16 was demonstrated to be exclusively expressed in the thick ascending limb of Henle in human kidneys, which was confirmed in

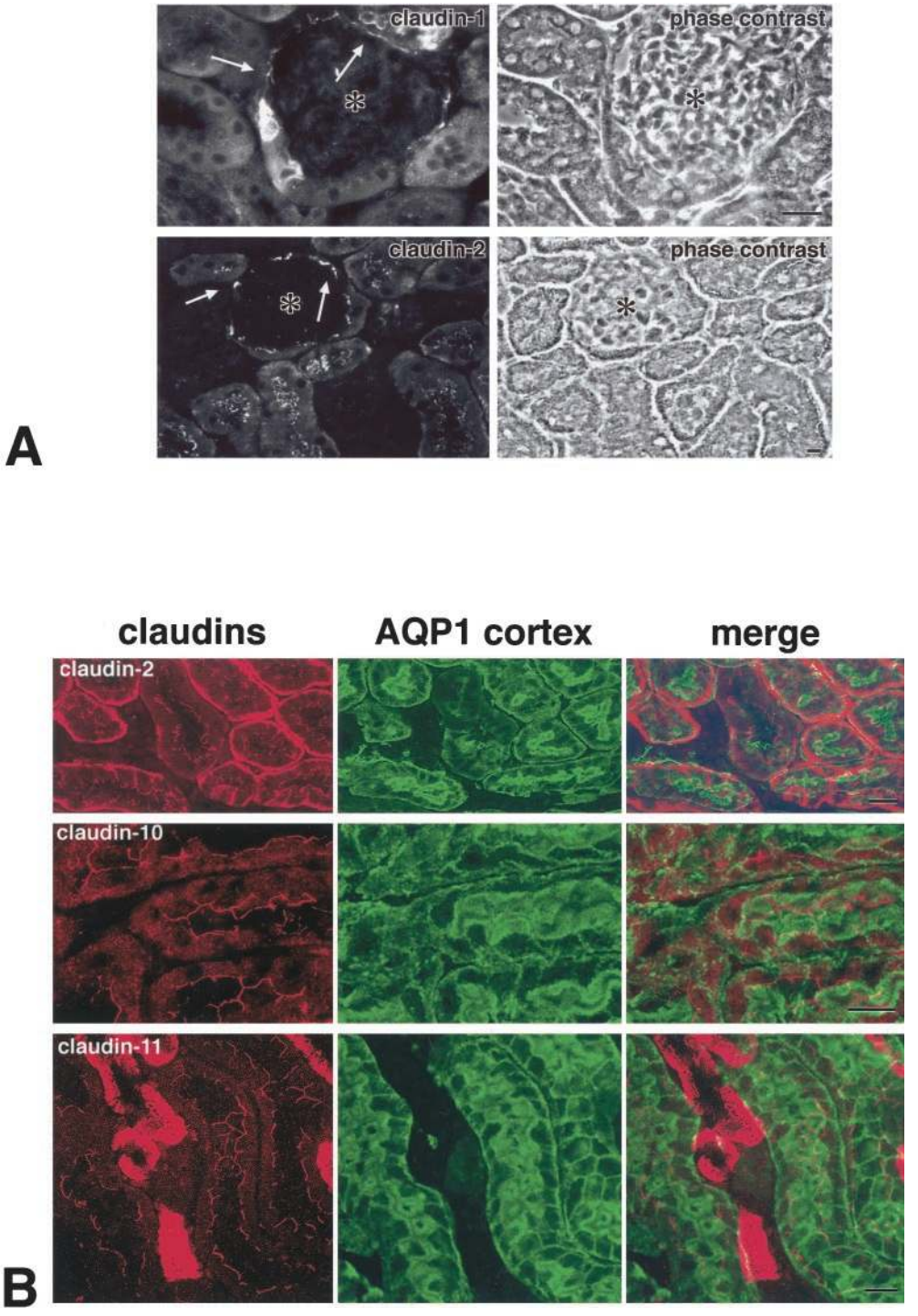

Figure 5. (A) Claudins expressed in Bowman's capsule. Claudin-1 and -2 were detected in Bowman's capsule (arrows), which was identified by comparison of an immunofluorescence image (left) with the corresponding phase-contrast image (right). Asterisks, glomeruli. Bars, 20 μm. (B) Claudins expressed in the proximal tubule. Claudin-2, -10, and -11 were concentrated at TJ of epithelial cells in proximal tubules (red), which were identified as AQP1-positive tubules in the cortex (green). Bars, 20 μm.

mouse kidneys in this study. This finding led to a very intriguing conclusion, namely that claudin-16 is directly involved in the selective paracellular conductance of Mg^{2+} ions in claudin-based TJ strands, with claudin-16 forming aqueous pores that function as paracellular Mg^{2+} channels within paired strands. It is possible that claudin-16 forms such pores via homotypic adhesion within paired strands. However, as we discussed previously (17), it is also possible that the weak heterotypic adhesion of claudin-16 to other claudin species results in the formation of aqueous pores with high conductance for Mg^{2+}

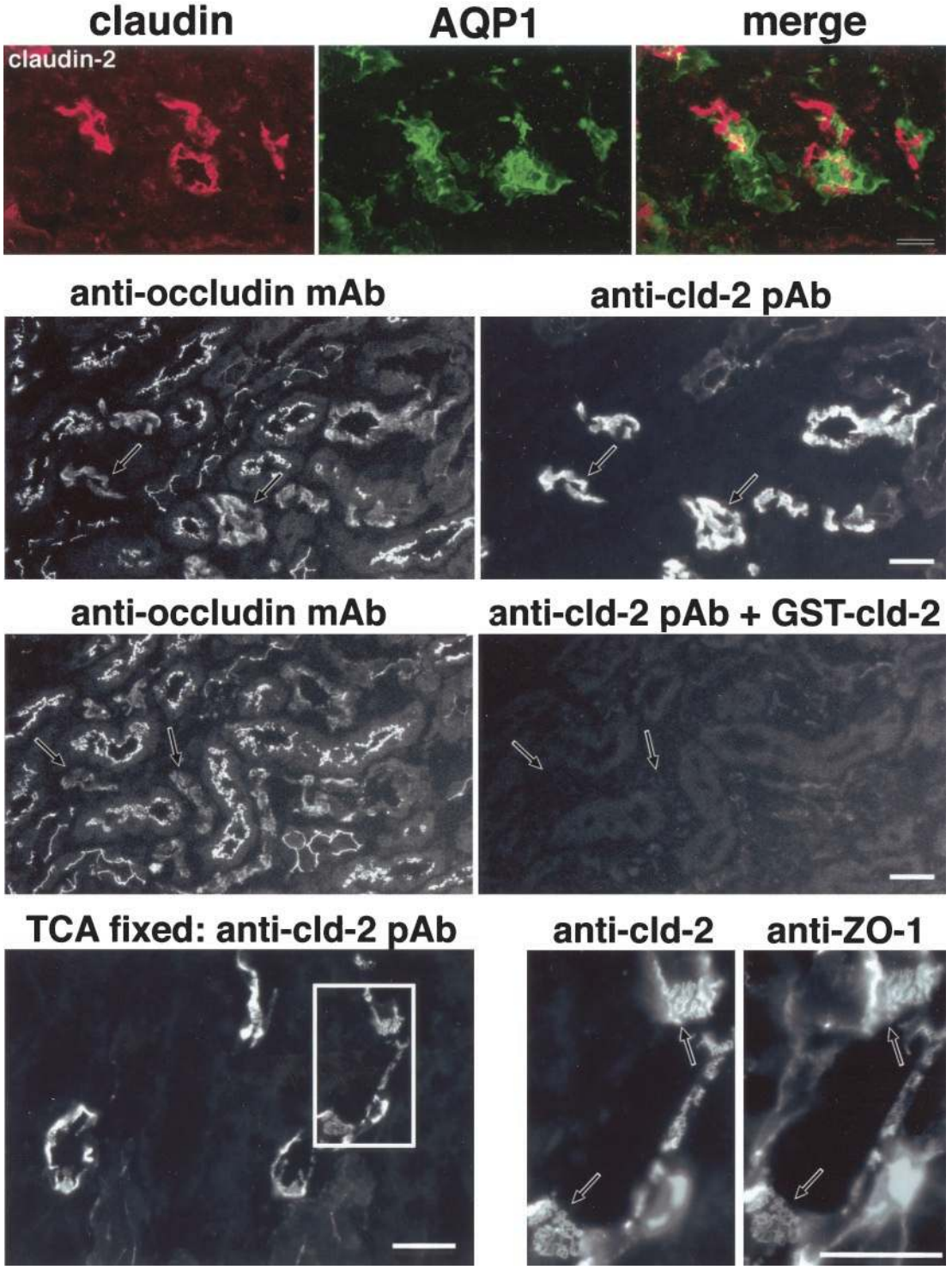

Figure 6. Claudins expressed in the thin descending limb of Henle. Only claudin-2 was detected in the thin descending limbs of Henle (red), which were identified as AQP1-positive tubules in the medulla (green). In these images, claudin-2 did not seem to be concentrated in TJ-like thin lines but was diffusely distributed in broad bands. Double staining with anti-occludin mAb and anti-claudin-2 pAb revealed that not only claudin-2 but also occludin seemed to be diffusely distributed in broad bands in the thin descending limb of Henle (arrows). This staining became undetectable when anti-claudin-2 pAb was pretreated with GST-claudin-2 (anti-cld-2 pAb + GST-cld-2, arrows). When the sections were fixed with TCA, similar diffuse claudin-2-staining was detected at low magnification (left), but close inspection (right, representing rectangle at left) revealed that individual sharp lines were intermingled within the claudin-2-positive zones (arrows). These lines were also Zomula Occludens-1-positive (occludin-positive) (arrows). Bars, 20 μm.

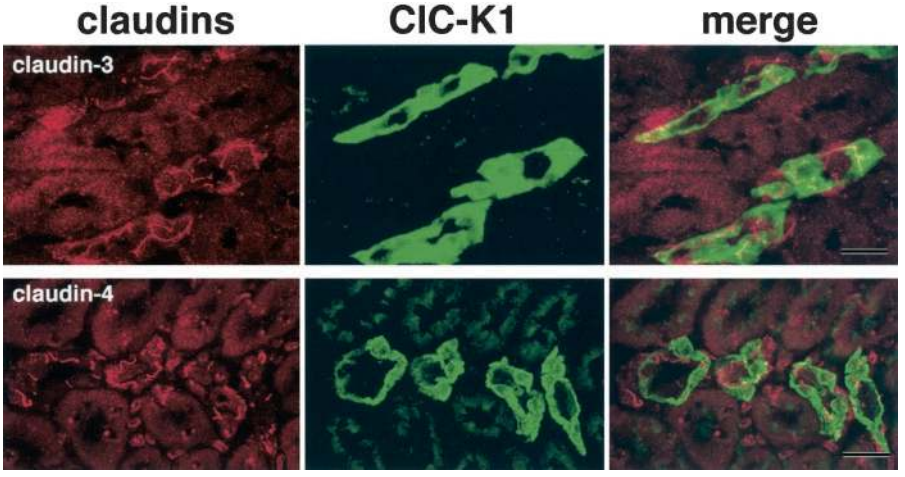

Figure 7. Claudins expressed in the thin ascending limb of Henle. In addition to claudin-8 (Figure 3), claudin-3 and -4 were concentrated at TJ of epithelial cells in the thin ascending limbs of Henle (red), which were identified as ClC-K-positive tubules (green). Bars, 20 μm.

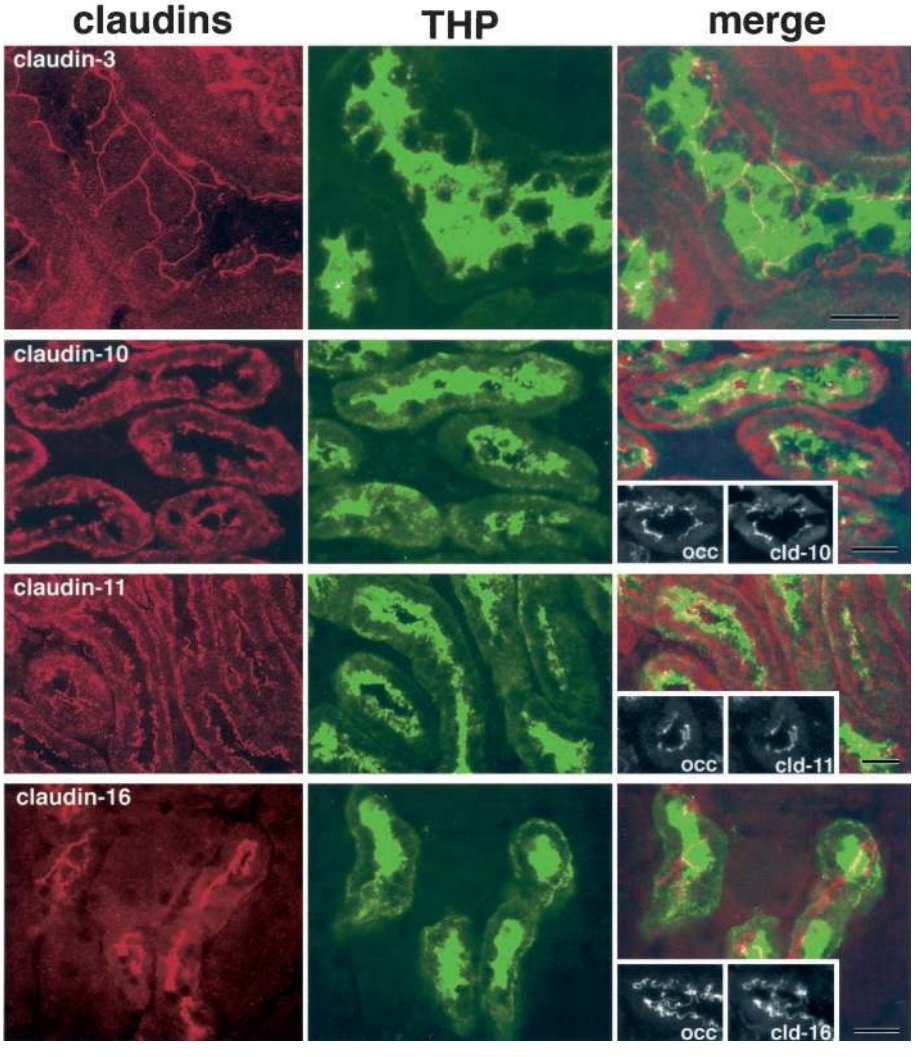

Figure 8. Claudins expressed in the thick ascending limb of Henle. Four distinct claudin species, namely claudin-3, -10, -11, and -16, were concentrated at TJ of epithelial cells in the thick ascending limbs of Henle (red), which were identified as THP-positive tubules (green). Insets, double immunostaining of transversely sectioned tubules with anti-occludin (occ) mAb and anti-claudin-10 (-11 or -16) (cld-10) pAb. The basal regions of these renal tubules were occasionally stained with anti-claudin-10 and -11 pAb but, as indicated by several control observations, this staining did not seem to be specific (insets). Bars, 20 μm.

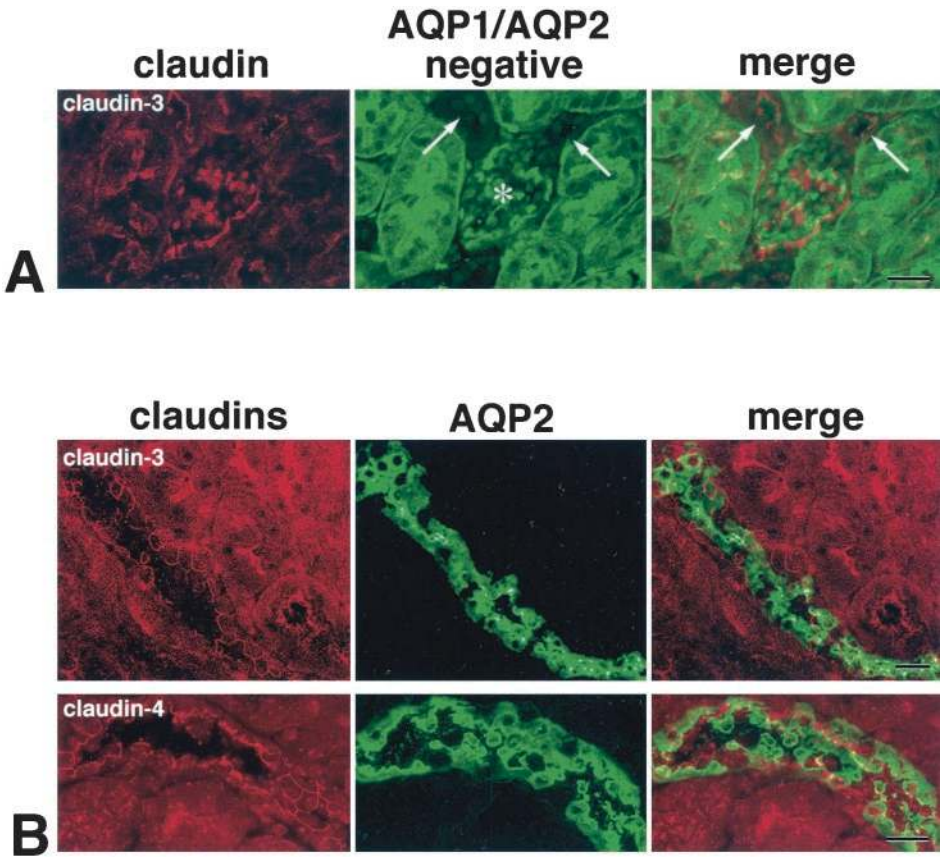

Figure 9. (A) Claudins expressed in the distal tubule. In addition to claudin-8 (Figure 3), claudin-3 was detected in TJ of distal tubules (red), which were identified as AQP1/2-double-negative tubules (arrows) located around glomeruli (asterisk). Double staining with anti-occludin mAb confirmed that these claudin-8 signals were derived from TJ (data not shown). Some signals seemed to be detected for glomeruli, including parietal epithelium, but control staining experiments (Figure 4) revealed that they were nonspecific. Bar, 20 μm. (B) Claudins expressed in the collecting duct. In addition to claudin-8 (Figure 3), claudin-3 and -4 were concentrated at TJ of epithelial cells in collecting ducts (red), which were identified as AQP2-positive tubules (green). Bars, 20 μm.

ions within the paired strands. As demonstrated in Figure 10, together with claudin-16, claudin-3, -10, and -11 constituted TJ strands in the thick ascending limb of Henle. Therefore, whether claudin-3, -10, or -11 is involved in the paracellular Mg^{2+} channels in collaboration with claudin-16 should be examined in the near future.

This study provides the first detailed description of the expression patterns of claudins in nephrons, but several questions remain unanswered. Notably, information regarding the distributions of claudin-7 and -12 in nephrons is still lacking. It is also possible that some of claudin-17 to -24 are expressed in nephrons. Indeed, although two to four distinct claudin species were coexpressed in most nephron segments, only claudin-2 was detected in the thin descending limb of Henle. It is possible that we overlooked the expression of other types of claudins in this segment.

The molecular mechanisms underlying material transport across renal epithelial cells via the transcellular pathway have been intensively analyzed. However, lack of information regarding the TJ-specific integral membrane proteins has hampered direct assessment, at the molecular level, of the molecular mechanism underlying paracellular flux across the renal epithelium. Claudins have been identified, and their patterns of expression in mouse nephron segments have been clarified. The results of this study can facilitate understanding not only of the physiologic functions of nephron segments but also of various pathologic states and diseases caused by alterations in the tightness of TJ in each nephron segment, in molecular terms.

Acknowledgments

We thank Dr. S. Sasaki (Tokyo Medical and Dental University, Tokyo, Japan) for generously donating anti-AQP2 pAb. Our thanks are also due to all of the members of our laboratory (Department of Cell Biology, Faculty of Medicine, Kyoto University) for helpful discussions. This study was supported in part by a Grant-in-Aid for Cancer Research and a Grant-in-Aid for Scientific Research (A) from the Ministry of Education, Science, and Culture of Japan (to Dr. Tsukita) and by a Japan Society for the Promotion of Science Research for the Future Program grant (to Dr. Furuse).

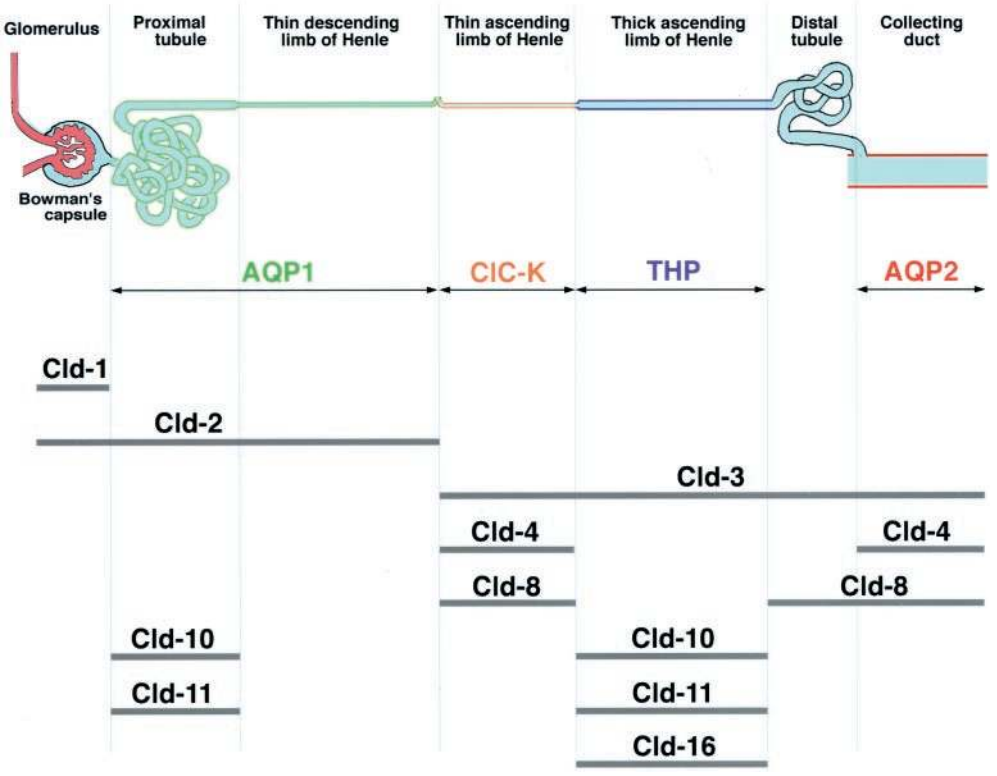

Figure 10. Summary of the segment-specific expression patterns of claudins in mouse nephrons. In the thin descending limb of Henle, some, but not all, AQP1-positive tubules were positive for claudin-2 (Cld-2). Similarly, from the thin ascending limb of Henle to the collecting duct, claudin-3 was detected in some, but not all, marker-positive tubules. These findings may be consistent with previous reports that the distal tubules, as well as the collecting tubules, are composed of several functionally distinct subsegments. In other cases, claudins were detected in all of the respective marker-positive tubules.

References

1. Anderson JM, van Itallie CM: Tight junctions and the molecular basis for regulation of paracellular permeability. *Am J Physiol* 269: G467–G475, 1995
2. Goodenough DA: Plugging the leaks. *Proc Natl Acad Sci USA* 96: 319–321, 1999
3. Tsukita S, Furuse M, Itoh M: Multifunctional strands in tight junctions. *Nature Rev Mol Cell Biol* 2: 285–293, 2001
4. Powell DW: Barrier function of epithelia. *Am J Physiol* 241: G275–G288, 1981
5. Reuss L: Tight junction permeability to ions and water. In: *Tight Junctions*, edited by Cereijido M, London, CRC Press, 1992, pp 49–66
6. Farquhar MG, Palade GE: Junctional complexes in various epithelia. *J Cell Biol* 17: 375–412, 1963
7. Staehelin LA: Further observations on the fine structure of freeze-cleaved tight junctions. *J Cell Sci* 13: 763–786, 1973
8. Staehelin LA: Structure and function of intercellular junctions. *Int Rev Cytol* 39: 191–283, 1974
9. Furuse M, Hirase T, Itoh M, Nagafuchi A, Yonemura S, Tsukita S, Tsukita S: Occludin: A novel integral membrane protein localizing at tight junctions. *J Cell Biol* 123: 1777–1788, 1993
10. Furuse M, Fujita K, Hiiragi T, Fujimoto K, Tsukita S: Claudin-1 and -2: Novel integral membrane proteins localizing at tight junctions with no sequence similarity to occludin. *J Cell Biol* 141: 1539–1550, 1998
11. Morita K, Furuse M, Fujimoto K, Tsukita S: Claudin multigene family encoding four-transmembrane domain protein components of tight junction strands. *Proc Natl Acad Sci USA* 96: 511–516, 1999
12. Tsukita S, Furuse M: Occludin and claudins in tight junction strands: Leading or supporting players? *Trends Cell Biol* 9: 268–273, 1999
13. Furuse M, Sasaki H, Fujimoto K, Tsukita S: A single gene product, claudin-1 or -2, reconstitutes tight junction strands and recruits occludin in fibroblasts. *J Cell Biol* 143: 391–401, 1998
14. Furuse M, Sasaki H, Tsukita S: Manner of interaction of heterogeneous claudin species within and between tight junction strands. *J Cell Biol* 147: 891–903, 1999
15. Furuse M, Furuse K, Sasaki H, Tsukita S: Conversion of zonulae occludentes from tight to leaky strand type by introducing claudin-2 into MDCK I cells. *J Cell Biol* 153: 263–272, 2001
16. Simon DB, Lu Y, Choate KA, Velazquez H, Al-Sabban E, Praga M, Casari G, Bettinelli A, Colussi G, Rodriguez-Soriano J, McCredie D, Milford D, Sanjad S, Lifton RP: Paracellin-1, a renal tight junction protein required for paracellular Mg^{2+} resorption. *Science (Washington DC)* 285: 103–106, 1999
17. Tsukita S, Furuse M: Pores in the wall: Claudins constitute tight junction strands containing aqueous pores. *J Cell Biol* 149: 13–16, 2000
18. Morita K, Sasaki H, Furuse M, Tsukita S: Endothelial claudin: Claudin-5/TMVCF constitutes tight junction strands in endothelial cells. *J Cell Biol* 147: 185–194, 1999
19. Morita K, Sasaki H, Fujimoto K, Furuse M, Tsukita S: Claudin-11/OSP-based tight junctions of myelinated sheaths of oligoden-

drocytes and Sertoli cells in testis. *J Cell Biol* 145: 579–588, 1999
20. Saitou M, Ando-Akatsuka Y, Itoh M, Furuse M, Inazawa J, Fujimoto K, Tsukita S: Mammalian occludin in epithelial cells: Its expression and subcellular distribution. *Eur J Cell Biol* 73: 222–231, 1997
21. Hirano T, Kobayashi N, Itoh T, Takasuga A, Nakamaru T, Hirotsune S, Sugimoto Y: Null mutation of PCLN-1/claudin-16 results in bovine chronic interstitial nephritis. *Genome Res* 10: 659–663, 2000
22. Chomczynski P, Sacchi N: Single-step method of RNA isolation by acid guanidinium thiocyanate-phenol-chloroform extraction. *Anal Biochem* 162: 156–159, 1987
23. Laemmli UK: Cleavage of structural proteins during the assembly of the head of bacteriophage T4. *Nature (Lond)* 227: 680–685, 1970
24. Hayashi K, Yonemura S, Matsui T, Tsukita S, Tsukita S: Immunofluorescence detection of ezrin/radixin/moesin (ERM) proteins with their carboxyl-terminal threonine phosphorylated in cultured cells and tissues: Application of a novel fixation protocol using trichloroacetic acids (TCA) as a fixative. *J Cell Sci* 112: 1149–1158, 1999
25. Enck AH, Berger UV, Yu AL: Claudin-2 is selectively expressed in proximal nephrons in mouse kidney. *Am J Physiol* 281: F966–F974, 2001
26. Agre P: Aquaporin water channels in kidney. *J Am Soc Nephrol* 11: 764–777, 2000
27. Yoshikawa M, Uchida S, Yamauchi A, Miyai A, Tanaka Y, Sasaki S, Marumo F: Localization of rat CLC-K2 chloride channel mRNA in the kidney. *Am J Physiol* 276: F552–F558, 1999
28. Vandewalle A, Cluzeaud F, Bens M, Kieferle S, Steinmeyer K, Jentsch TJ: Localization and induction by dehydration of ClC-K chloride channels in the kidney. *Am J Physiol* 272: F678–F688, 1997
29. Hession C, Decker JM, Sherblom AP, Kumar S, Yue CC, Mattaliano RJ, Tizard R, Kawashima E, Schmeissner U, Heletky S, Chow EP, Burne CA, Shaw A, Muchmore AW: Uromodulin (Tamm-Horsfall glycoprotein): A renal ligand for lymphokines. *Science (Washington DC)* 237: 1479–1484, 1987
30. Fushimi K, Uchida S, Hara Y, Hirata Y, Marumo F, Sasaki S: Cloning and expression of apical membrane water channel of rat kidney collecting tubule. *Nature (Lond)* 361: 549–552, 1993
31. Schwartz MM, Venkatachalam MA: Structural differences in thin limbs of Henle: Physiological implications. *Kidney Int* 6: 193–208, 1974
32. Fasth A, Hoyer JR, Seiler MW: Renal tubular immune complex formation in mice immunized with Tamm- Horsfall protein. *Am J Pathol* 125: 555–562, 1986
33. Rahner C, Mitic LL, Anderson JM: Heterogeneity in expression and subcellular localization of claudins 2, 3, 4, and 5 in the rat liver, pancreas, and gut. *Gastroenterology* 120: 411–422, 2001
34. Stevenson BR, Anderson JM, Goodenough DA, Mooseker MS: Tight junction structure and ZO-1 content are identical in two strains of Madin-Darby canine kidney cells which differ in transepithelial resistance. *J Cell Biol* 107: 2401–2408, 1988
35. Lutz MD, Cardinal J, Burg MB: Electrical resistance of renal proximal tubule perfused *in vitro*. *Am J Physiol* 225: 729–734, 1973
36. Boulpaep E, Seely JF: Electrophysiology of proximal and distal tubules in the autoperfused dog kidney. *Am J Physiol* 221: 1084–1096, 1971
37. Claude P, Goodenough DA: Fracture faces of zonulae occludentes from "tight" and "leaky" epithelia. *J Cell Biol* 58: 390–400, 1973